MAPPING COHERENT, TIME-VARYING WAVEFRONTS FROM THE 2011 TOHOKU TSUNAMI INTO ENHANCED, TIME-DEPENDENT WARNING MESSAGES

J. Shi[1], M. D. Kohler[2], J. N. Sutton[3], J.-P. Ampuero[4]

(1) Ph.D. student, Department of Mechanical and Civil Engineering, California Institute of Technology, jian.shi@caltech.edu

(2) Research Assistant Professor, Department of Mechanical and Civil Engineering, California Institute of Technology, kohler@cal-tech.edu

(3) Assistant Professor, Department of Communication, University of Kentucky, jeannette.sutton@uky.edu

(4) Professor of Seismology, Seismological Laboratory, California Institute of Technology, ampuero@gps.caltech.edu

Abstract

Recent results are presented to illustrate how predictions of tsunami wave impact and tsunami warning messages can be improved by including information about multiple, large-amplitude wave arrivals over longer time durations and at refined spatial resolution. A deployment of ocean bottom seismometers off the coast of southern California recorded the March 2011 Tohoku tsunami on 22 differential pressure gauges. The pressure gauge tsunami records across the entire array show multiple large-amplitude, coherent phases arriving one hour to more than 36 hours after the initial tsunami phase. Analysis of the pressure gauge recordings reveals possible locations of the geographical sources that contributed to secondary tsunami arrivals in southern California. A beamforming technique is applied to the pressure gauge data to determine the azimuths and arrival times of scattered wave energy. In addition, a backward ray-tracing procedure is applied to a wide range of back azimuth starting values from the pressure gauge array to map possible scattering source locations. The results show several possible candidates of secondary tsunami source structures. These include: (1) southeastern Alaska producing a tsunami arrival 1–2 hours after the first arrival; and elongated bathymetry structures near: (2) the northern Hawaiian Island chain producing an arrival 1–2 hours, (3) Papua New Guinea producing an arrival 8–9 hours, and (4) French Polynesia producing an arrival 10–11 hours, all after the first arrival. These results are then incorporated into tsunami warning messages to improve clarity of the hazard threat and protective action guidance, and the specificity of impact location over time. Revised tsunami messages have been tested through online experiments with the public in order to determine how changes in message clarity and specificity affects message receiver understanding, believing, and personalizing, all of which are pre-decisional sense-making activities. The geophysical results are mapped into modified tsunami warning messages to show how a time-varying hazard could be communicated with more effective message format and content. The results are demonstrating the effects of including clearly described locations, time of impact, and hazard impact consequences on message perception among the public.

Keywords: tsunami, beamforming technique, coherence stacking, back projection, tsunami warning

1. Introduction

The March 11, 2011 M_w 9.0 Tohoku Japan earthquake resulted in a major tsunami that propagated across the Pacific Ocean. A few months earlier in late 2010, the temporary ALBACORE (Asthenospheric and Lithospheric Broadband Architecture from the California Offshore Region Experiment) array of ocean bottom seismometers (OBS) and differential pressure gauges (DPG) was deployed off the coast of southern California (Fig. 1), where it recorded the Tohoku tsunami with unprecedented spatial and temporal resolution [1, 2]. This OBS array spanned a region that was 150 km north-south by 400 km east-west, extending into the deep open Pacific Ocean west of the edge of the continental shelf. In this array (Fig. 1), 22 stations with an average spacing of 75 km were equipped with DPGs that recorded water pressure waveform time series data continuously at 50 samples per second (DPGs are designed specifically to record low-frequency pressure data with high fidelity [3]). Such spatial and temporal resolution of the data, enabled only by a dense configuration like the ALBACORE array, made it possible to investigate features in the tsunami waveforms which have not previously been observed with this level of clarity at this spatial scale. By contrast, the Deep-ocean Assessment and Reporting of Tsunamis (DART) buoy system designed by National Oceanic and Atmospheric Administration (NOAA) [4, 5] has a much larger station spacing, precluding it from recording waveforms that show multiple and coherent scattered wave arrivals. The ALBACORE dataset presents a rare opportunity to incorporate analysis results of field hazard recordings into tsunami models that lead to enhanced tsunami warning messages. While improvements in DART technology are now resulting in real-time refinements to the forecasts from multiple sensors, the extremely large station spacing precludes the DART network from being used to validate complex, coherent features in modeled tsunami waveforms.

Our analysis of the ALBACORE data is motivated by recent studies that have applied array processing methods to relatively dense seismic arrays for different purposes. For example, Zhang et al. [6] studied oceanic storms; Meng et al. [7] used USArray and European seismic data to image the rupture process of the Tohoku earthquake; and Traer et al. [8] estimated the incidence direction of microseismic noise. Methods used are either beamforming, back-projection, or the two combined. These results demonstrate the effectiveness of the array analysis methodology, inspiring us to process our data using analogous approaches as our starting point. Back-projection has been previously applied to tsunami data, but without exploiting waveform coherency through array processing. For instance, Heidarzadeh et al. [9] applied backward tsunami ray tracing to a widely spaced set of tide gauge and DART records to locate a tsunami source. Array processing techniques have been previously applied to seafloor pressure data recorded by small-aperture arrays to estimate the direction of arrival of tsunami waves [10] and to study infragravity waves [11]. Tsunami recordings by dense arrays of seafloor pressure sensors may become increasingly available in the future (e.g. [12]). The present study demonstrates how array processing can provide critical information about the tsunami wave characteristics from such data.

Fig. 2 shows the waveforms recorded by the ALBACORE DPG array. These clearly show multiple, large-amplitude, coherent phases arriving between one hour and more than 24 hours after the first tsunami arrival. This wave energy scattering phenomenon has been observed in past numerical simulation results [13, 14, 15], and was associated with wave scatterers in the Pacific Ocean which are primarily uneven topographic features such as the Emperor Seamount Chain, the Hawaiian Ridge and Islands, and French Polynesia [16, 17]. These scatterers reflect or refract tsunami waves, act as secondary point sources or wave guides, and redirect and redistribute tsunami wave energy within the ocean.

Our overarching goal in this study is to identify the scatterers that contributed to the subsequent coherent phases arriving after the first tsunami arrival, and to use these findings in the development of next-generation, time-sensitive warning messages along any coastline for future tsunamis. To this end, we first utilize array beamforming techniques which are based solely on the array-recorded waveforms and not the source or the path information. Specifically, we apply a correlation stacking technique (similar to what was utilized in [18, 19, 20]) by time-shifting tsunami waveforms such that components incident with a given azimuth and for a given slowness result in the highest average waveform coherence across the array. Then, we use a back-projection (backward ray-tracing) technique (similar to that of [9]) to numerically backward-trace tsunami propagation simulation results obtained by the Tsunami Travel Time (TTT) software package [21].

Using beamforming together with backward ray tracing, we identify topographic scatterers most likely to have

caused the multiple wave arrivals. These include: (1) southeast Alaska producing a tsunami arrival 1–2 hours after the first arrival; and elongated bathymetry structures near (2) the northern Hawaiian Island chain producing an arrival 1–2 hours, (3) Papua New Guinea producing an arrival 8–9 hours, and (4) French Polynesia producing an arrival 10–11 hours after the first arrival.
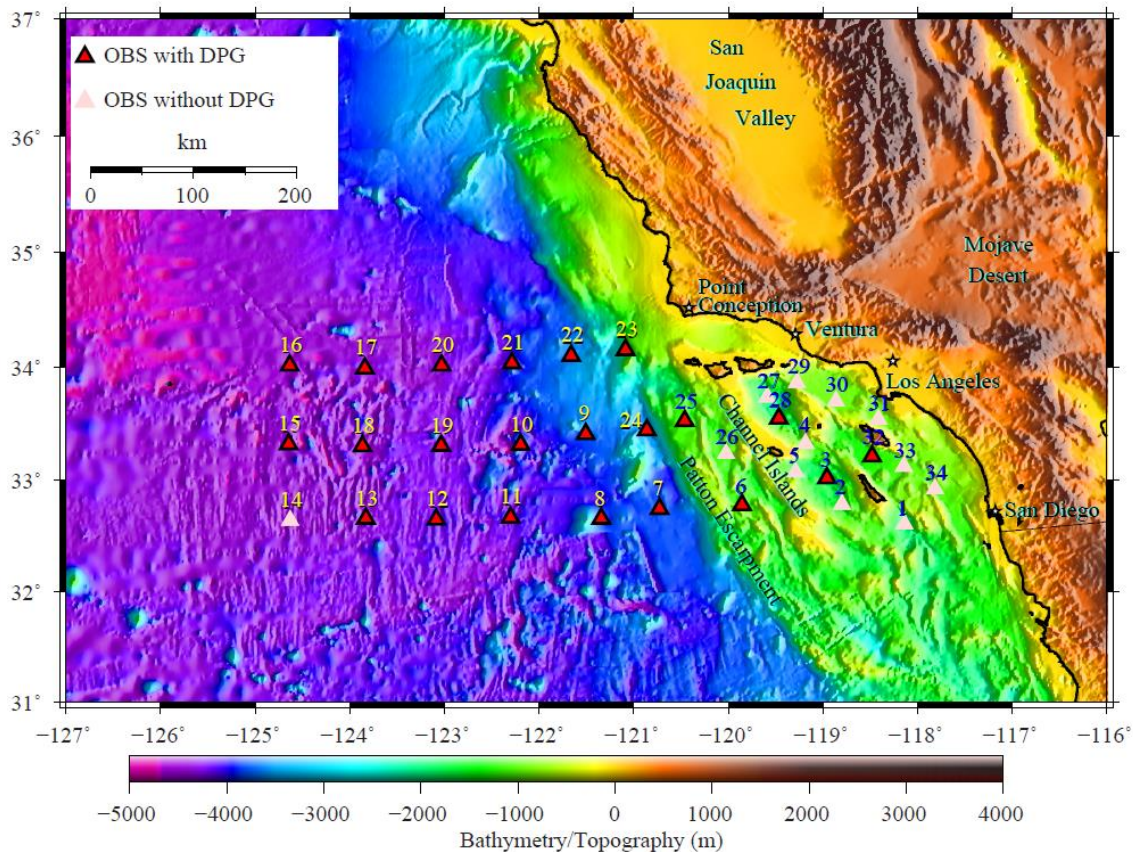

Fig. 1: Map showing the 22 recovered ALBACORE stations with differential pressure gauge (DPG) sensors (red triangles) that recorded the 2011 Tohoku tsunami (modified from [22]). Bathymetry is ETOPO1 [23].

2. Array beamforming: methods and results

We utilize an array beamforming technique, more specifically the "correlation stacking" utilized in [20] to process the recorded tsunami waveforms. First, we exclude eight stations in the array that were on the continental shelf (east of the Patton Escarpment in Fig. 1) out of the total 22 stations. This is to avoid additional complexity and bias due to local scattering sources such as nearby islands, irregularities in the southern California coastline, and the abrupt bathymetry gradient introduced at the Patton Escarpment.

The waveforms are bandpass filtered in two period bands: 7–9 min and 15–17 min. These two period bands correspond to wavelengths of ~93 km and ~189 km, respectively, and are the characteristic length scales of smaller scatterers (i.e., single islands or seamounts) and larger scatterers (i.e., elongated island or seamount chains).

Next, a grid search is performed in the slowness space (slowness = 1/velocity) comprising the two components of the slowness vector (S_E, S_N), east-west and north-south, respectively. For each (S_E, S_N) pair we time-shift the filtered waveforms according to a plane wave model and then calculate the "stacked correlation coefficient" (scc) defined as the sum of the normalized cross-correlation coefficients of all station pairs ([20]). This procedure is applied to sliding windows whose length is three times the center period of the filter band. Fig. 3 shows the scc of a selected time window as a function of S_E and S_N for the two period bands. The higher the scc, the more likely the

tsunami wave arrives with an identifiable east-west velocity $1/S_E$ and north-south velocity $1/S_N$, enabling us to calculate the arriving azimuth (computed in degrees from north) of the incoming wave.
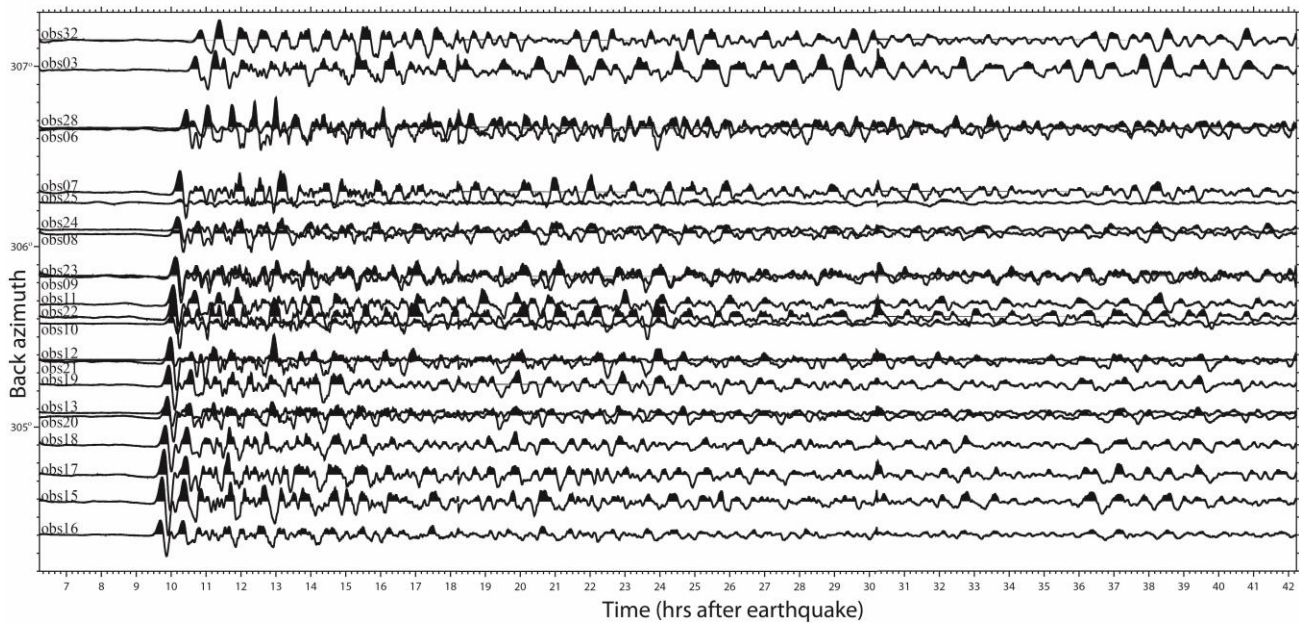

Fig. 2: The 2011 Tohoku tsunami waveforms recorded by the ALBACORE DPG array offshore southern California. Amplitude scale is the same for all waveforms. Positive polarities are shaded.

Fig. 3 shows multiple (S_E, S_N) pairs with high *scc* (hereafter referred to as "hot spots") aligned in a regular pattern. Spurious hot spots can result from aliasing if the wavelength associated with the period band is comparable or smaller than the array station spacing. The ALBACORE array station spacing is ~75 km, and the wavelength of the 7–9 min band is approximately 93 km; thus the 7-9 min result (Fig. 3a) exhibits obvious aliasing that hinders the identification of the correct incoming azimuth of a wave.

To remove the effects of aliasing, the search for the correct hot spot is constrained to a narrow slowness annulus that corresponds to the tsunami velocity for the specific period band. For example in Fig. 3a, the theoretical tsunami velocity for the period band 7–9 min is 0.195 km/s, i.e., slowness = 5.13 s/km [24], using the averaged depth of the 14 ALBACORE sites. Thus only the hot spots on the dashed ring in Fig. 3a indicate true incoming tsunami waves and all other hot spots are the results of aliasing. Fig. 3b shows two hot spots on the dashed ring, both of which indicate true tsunami arrivals.

Note that Fig. 3 only shows the *scc* of one specific time window. For each sliding window, we compute the *scc* and extract the *scc* values along the dashed ring (such as in Fig. 3). We then plot together the *scc* values extracted for all time windows as a function of time and azimuth, as shown in Fig. 4.

Fig. 4 shows different hot spots corresponding to different wave arrival times and arrival azimuths. The first of these hot spots occurs at ~9.6 hours after the earthquake origin time at an azimuth of ~305°; this is the first (direct) tsunami arrival. Additional hot spots in both period bands are identified. The more distinct they are, the more likely they are the result of a coherent wave arrival from a distant scattering source. We have identified, at this point, three subsequent coherent arrivals that we describe further in the next section: (1) 1–2 hours after the initial arrival (11–12 hours after the earthquake) with azimuth 275°–300°, seen in both period bands; (2) 8–9 hours after the initial arrival with azimuth 275°–300°, only seen in the 15–17 min band; (3) 10–11 hours after the initial arrival with azimuth 215°–230°, only seen in the 15–17 min band.

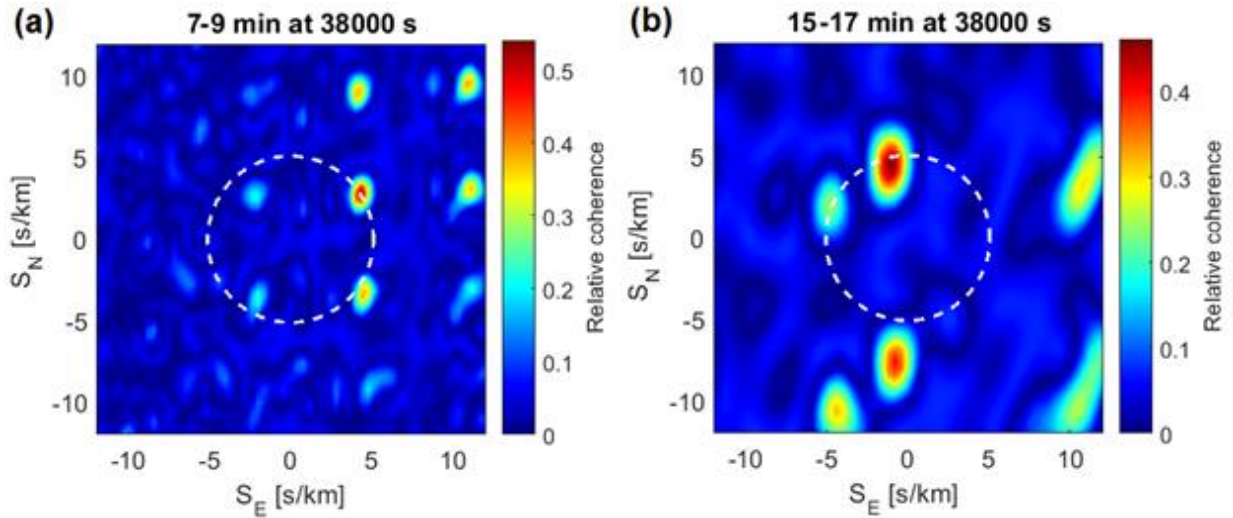Fig. 3: Stacked correlation coefficient as a function of east-west slowness (S_E) and north-south slowness (S_N) for (a) 7–9 min period filter band and (b) 15–17 min period filter band at 38,000 s (~10 hr) after the earthquake origin time.
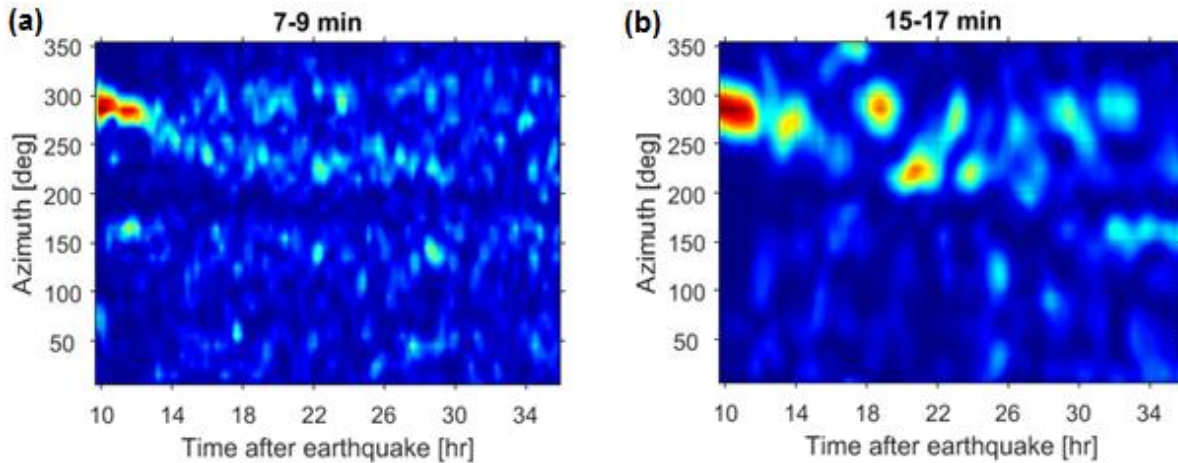

Fig. 4: Stacked correlation coefficient as a function of arrival time and azimuth of incoming wave for the (a) 7-9 min, and (b) 15-17 min period filter bands. The horizontal axes show time after earthquake origin time; the first tsunami arrival was ~9.6 hours after the earthquake origin time.

3. Back projection: methods and results

We next use the information from the three coherent arrivals obtained in the previous section to identify the actual geographic locations of the scatterers that may have produced them. We use a back-projection, ray-tracing technique, similar to that used by [9], to trace the tsunami wave from the ALBACORE array to the scattering source.

First we compute the travel times of a virtual tsunami that originates from the center point of the 14 deep-water, open ocean ALBACORE stations using the Tsunami Travel Time (TTT) software package [21]. TTT uses the long-wave (shallow water) assumption and solves for the travel times of the propagating wavefront using Huygens principle for a user-specified bathymetry model (e.g. [23]). However, since this approach assumes a ray approximation, we must first account for the fact that the width of our filtered tsunami rays is not infinitely small and the filtered tsunami wave travel times will be affected by bathymetry features as large as the wavelengths corresponding to the

period filter bands (i.e., finite-frequency effects). We thus smooth ETOPO1 [23] bathymetry to the appropriate length scales corresponding to the two period bands (in fact, we convert water depth to wave slowness, and smooth the slowness values). We then use the two smoothed bathymetry models as input to TTT to obtain the tsunami travel-time field for the Pacific Ocean. Fig. 5 shows the original ETOPO1 bathymetry model, bathymetry smoothed to a length scale corresponding to the 7–9 min band, and bathymetry smoothed to a length scale corresponding to the 15–17 min band. Fig. 5 shows how the different smoothing procedures highlight different seafloor features and amplitudes, indicating how they will each result in different tsunami travel times.
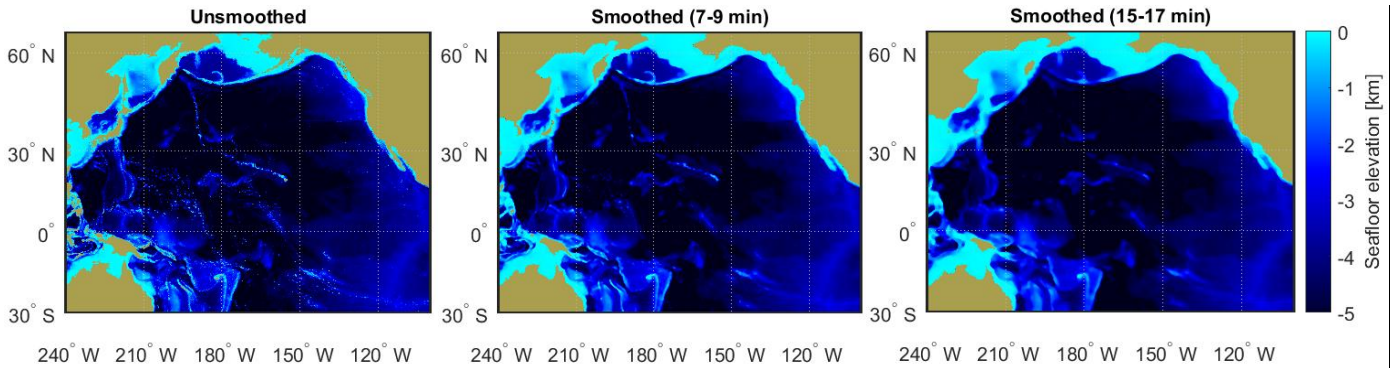

Fig. 5: ETOPO1 [23] bathymetry maps smoothed to different length scales. Left: Original, unsmoothed. Center: Smoothed to length scale corresponding to 7–9 min filter band. Right: Smoothed to length scale corresponding to 15–17 min filter band.

We next compute the gradient of the travel time to produce the velocity field. We start the ray tracing from the virtual tsunami origin point (center of the ALBACORE array), making a small step in the direction of the azimuth of a selected hot spot identified in the previous section. We evaluate the new ray direction at the end of the step by interpolating the computed velocity field, and then make a new step. We iterate this procedure. The end result is a backward-traced ray corresponding to a specified azimuth of arrival at ALBACORE. We repeat the ray tracing for a range of azimuths spanning the uncertainty of our array processing estimates, and for each significant hot spot.

3.1 Coherent arrival 1-2 hours after the direct tsunami arrival

We use nine take-off azimuths in the range of 275°–300° (with increments of 3°) corresponding to the first coherent arrival 1–2 hours after the direct arrival (as indicated in Fig. 4). The ray-tracing procedure is stopped at 2 hr, which is the arrival time of the next coherent arrival. Fig. 6 shows the back-projection ray-tracing results. The star denotes the center of the ALBACORE array and the colored lines denote the different rays corresponding to the different take-off azimuths. The starting point of these rays is the ALBACORE array, and the rays end at the location where 2 hours of "excess travel time" is reached. The "excess travel time" is a scalar field defined for every (x,y) location in the ocean by

$$T_{excess}(x,\ y) = T_{total}(x,\ y) - T_{direct} \tag{1}$$

where $(x,\ y)$ are longitude/latitude coordinates, T_{direct} is the direct tsunami travel time from the earthquake epicenter to the ALBACORE array (approximately 9.6 hours), and $T_{total}(x,\ y)$ is the travel time of a tsunami wave scattered at $(x,\ y)$, i.e. the sum of the tsunami travel time from the epicenter to $(x,\ y)$ and then from $(x,\ y)$ to the ALBACORE array. Hence

$$T_{total}(x,\ y) = T_{forward}(x,\ y) + T_{backward}(x,\ y) \tag{2}$$

where $T_{forward}(x,\ y)$ and $T_{backward}(x,\ y)$ are two travel-time fields computed forward from Tohoku to (x,y), and backward from ALBACORE to (x,y), respectively. With this definition, $T_{excess}(x,\ y) = 2$ hours indicates a tsunami arrival 2 hours after the direct arrival (T_{direct}).

We then cross reference the end points of the backward-traced rays with the bathymetry features, and manually identify the regions that most likely contributed to a particular coherent arrival. Our theoretical basis for associating a bathymetry feature as a potential scattering source is independently supported from studies by Mofjeld et al. [16, 17], in which a tsunami scattering index (TSI) is defined and associated with the irregularity of the bathymetry. They have found that the more irregular the bathymetry within a particular region (compared to adjacent surrounding regions), the higher the TSI value, and thus the higher the probability that the region can scatter tsunami energy.

Fig. 6a shows that two regions may be associated with the 1-2 hours coherent arrival: (1) Hawaiian Island chain, and (2) the coast of southeastern Alaska, indicated by the two thicker rays. The former (Hawaiian Islands) acts as a refractor and the latter (Alaskan coastline) acts as a reflector. Due to the spatial resolution limits of the beamforming results (determined by the minimum station spacing in the ALBACORE array), we cannot differentiate the two source regions from the available recordings; thus we list both as equally likely candidates.

3.2 Coherent arrival 8-9 hours after the direct tsunami arrival

Using the same method described above, we computed the backward ray-tracing travel-time field for the second subsequent arrival: T_{excess} = 8–9 hours, with an azimuth range of 275°–300°, shown in Fig. 6b. These rays follow the exact same path as in Fig. 6a, but extend much further because T_{excess} is now larger. For this case we identify Papua New Guinea as the likely scatterer, indicated by the two thicker rays in Fig. 6b. Note that these two rays propagate past the Hawaiian Island chain because in the smoothed bathymetry model corresponding to 15–17 min, the Hawaiian Island chain is an elongated, smoothed, submerged structure. This could also be the reason for the absence of a coherent arrival at T_{excess} = 8–9 hours for the 7–9 min band (Fig. 4a); the rays were stopped by the island chain.

3.3 Coherent arrival 10-11 hours after the direct tsunami arrival

Fig. 6c shows results for the third subsequent coherent arrival corresponding to T_{excess} = 10-11 hours, with an azimuth range of 275°–300°. The thick ray suggests that the bathymetry features at and around French Polynesia are a candidate for scattering of tsunami waves.
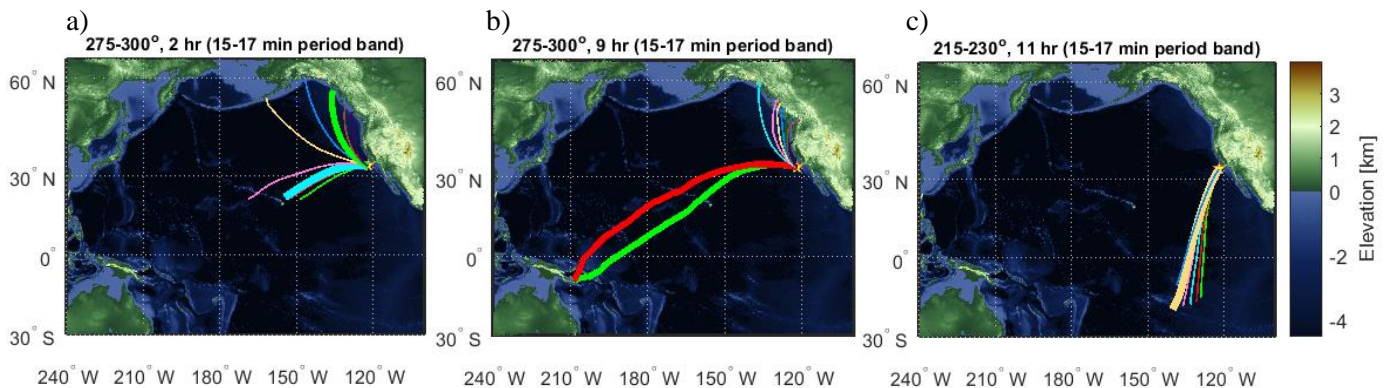

Fig. 6: Back-projected ray paths for the 15-17 min period band. a) The first subsequent coherent arrival (1–2 hours after the direct arrival). b) The second subsequent coherent arrival (8–9 hours after the direct arrival). c) The third subsequent coherent arrival (10–11 hours after the direct arrival).

Social science impact

The geophysical findings in tsunami-earthquake research described above are combined with findings from empirical social science research on public responses to warnings to develop enhanced tsunami warning messages. The enhanced messages increase specificity of geo-location, time to impact, and hazard impact consequences in order to improve appropriate protective action taking among members of the public. The intent of a warning message is to persuade individuals that they are not safe and to incite them to take actions to protect themselves and others. This is an inherent challenge, as individuals routinely believe that they are not at risk. Therefore, warning messages, along with other social and contextual factors, play a significant role in changing an individual's perception of risk. Findings from empirical research have demonstrated that effective warnings, that is, those that produce changed risk perceptions and persuade individuals to act, must be understood, believed, and made personal in order to increase the likelihood that an individual will take protective action. To do so, messages must include content that describes the hazard and its impact, the location of impact, the actions that an individual must do to keep safe, the time by which to take action, and the source of the message sender. Contents should be delivered in language that is clear, specific, consistent, and certain. Once an individual receives a message, they routinely seek additional confirmatory information or share that information with others before making a decision to act [25].

To date, little attention has been directed to public understanding and behavioral intent in response to tsunami warning messages [26]. Recent research focused on stakeholder perceptions of Tsunami Warning Center (TWC) products, and resulted in suggestions for more clearly stated contents and message reorganization [27, 28]. Populations with little knowledge of tsunamis (such as how a tsunami "works," its potential impact, and what they can do to protect themselves) including non-coastal residents such as vacationers, represent a high risk group for which it is important to consider their knowledge about protective actions and perceptions of tsunami risk. Therefore, we conducted focus groups with members of the public who are unfamiliar with tsunamis in order to assess their response to a National Weather Service (NWS) message distributed during the Tohoku tsunami (Fig. 7). The focus groups were audio recorded, transcribed, and coded for thematic content related to message understanding, believing, and personalization, paying attention to the areas of the message that were unclear or lacked specificity, and their interpretation of tsunami impacts that affect their decision making. We found that individuals consistently believed the message, but differed in their understanding of the hazard, its potential impact, the location of impact, and who should take action. Furthermore, many participants had a difficult time personalizing the threat due to a lack of location awareness and specificity of geographical areas of warning.

From the focus group findings, we developed revised tsunami messages that increased message specificity about location, potential impact, time of impact, and protective action guidance (Fig. 8). In addition, we provided information about what a tsunami threat is and what to watch for during a tsunami. The original message and the revised message, plus a 140-character message (Fig. 9) and a sequence of 140-character messages (Fig. 10), were tested in online experiments with a sample of 400 respondents. The 140-character message represents a short message that might be sent to a mobile phone or through an online social network, such as Twitter. The sequence of 140-character messages represents the revised tsunami message, disseminated in a format that could be received on a mobile phone or through an online social network, but increases the amount of content delivered in comparison with a single 140-character message. We conducted ANOVA (Analysis of Variance) to test the null hypothesis, that there would be no changes in outcome measures for the different messages. In comparison with the original message, preliminary results suggest the revised and sequenced message have positive effects for message understanding, personalizing, and believing, demonstrating that the changes in message specificity positively affected message interpretations. Preliminary analyses also suggest that the single, 140-character message resulted in negative perceptual outcomes, with reduced understanding, personalizing, and believing in comparison with the other three messages.

WWUS86 KEKA 111820
SPSEKA
SPECIAL WEATHER STATEMENT
NATIONAL WEATHER SERVICE EUREKA CA
1020 AM PST FRI MAR 11 2015

CAZ001-002-120030-
REDWOOD COAST-MENDOCINO COAST-
1020 AM PST FRI MAR 11 2015

...A TSUNAMI WARNING REMAINS IN EFFECT FOR DEL NORTE...HUMBOLDT AND MENDOCINO COUNTIES COASTAL AR-
EAS...

EARTHQUAKE DATA. PRELIMINARY MAGNITUDE 8.9. LOCATION 38.2 NORTH 142.5 EAST. NEAR EAST COAST OF HONSHU
JAPAN. TIME 21:46 PST MAR 10, 2015. A TSUNAMI WAS GENERATED AND HAS CAUSE DAMAGED ALONG THE DEL NORTE
COUNTY, AND DAMAGE ALONG THE HUMBOLDT AND MENDOCINO COASTS IS STILL EXPECTED. PERSONS AT THE COAST
SHOULD BE ALERT TO INSTRUCTIONS FROM LOCAL EMERGENCY OFFICIALS.

DAMAGING WAVES HAVE BEEN OBSERVED ACROSS HAWAIIAN ISLANDS. DAMAGING WAVES HAVE ARRIVED AT CRES-
CENT CITY HARBOR WHERE ALL DOCKS HAVE BEEN DESTROYED. WAVES HAVE BROKEN OVER THE SPIT AT STONE LA-
GOON. A 3-FOOT WAVE HAS BEEN REPORTED IN HUMBOLDT BAY. A 2-4 FOOT FLOOD WAVE WAS REPORTED MOVING UP
THE MAD RIVER AT 08:45 AM PST. DAMAGING WAVES WILL CONTINUE FOR THE NEXT SEVERAL HOURS.

MEASUREMENTS OR REPORTS OF TSUNAMI WAVE ACTIVITY GAUGE LOCATION TIME AMPLITUDE
CRESCENT CITY, CA 08:44 AM 8.1 FT, NORTH SPIT HUMBOLDT 8:30 AM 3.1 FT, ARENA COVE 09:17 AM 5.3 FT.

REMEMBER...DON'T BE FOOLED...TSUNAMI WAVES CAN SEEM STOP FOR LONG PERIODS AND THEN BEGIN AGAIN. WAIT
FOR THE OFFICIAL ALL CLEAR TO RETURN TO THREATENED AREAS.

IN DEL NORTE COUNTY...PEOPLE ARE ORDERED TO EVACUATE TO ABOVE 9TH STREET. SHELTER LOCATIONS INCLUDE
SMITH RIVER ELEMENTARY...DEL NORTE HIGH SCHOOL AND YUROK TRIBAL OFFICE IN KLAMATH.

IN HUMBOLDT AND MENDOCINO COUNTIES...PEOPLE ARE ADVISED TO STAY OFF BEACHES...NOT TRAVEL BY WATER-
CRAFT AND EVACUATE LOW LYING COASTAL AREAS IMMEDIATELY UNTIL ADVISED THAT IT IS SAFE TO RETURN.

PEOPLE SHOULD STAY CLEAR OF LOW LYING AREAS ALONG COASTAL RIVERS AS TSUNAMI WAVES CAN TRAVEL UP FROM
THE MOUTH OF COASTAL RIVERS.

BULLETINS WILL BE ISSUED HOURLY OR SOONER IF CONDITIONS WARRANT TO KEEP YOU INFORMED OF THE PROGRESS
OF THIS EVENT. IF AVAILABLE...REFER TO THE INTERNET SITE HTTP://TSUNAMI.GOV FOR MORE INFORMATION.

DUE TO RAPIDLY CHANGING CONDITIONS ASSOCIATED WITH TSUNAMI WAVE ACTIVITY...LISTENERS ARE URGED TO TUNE
TO LOCAL EMERGENCY ALERT SYSTEM MEDIA FOR THE LATEST INFORMATION ISSUED BY LOCAL DISASTER PREPARED-
NESS AU-THORITIES. THEY WILL PROVIDE DETAILS ON THE EVACUATION OF LOW-LYING AREAS...IF NECESSARY...AND
WHEN IT IS SAFE TO RETURN AFTER THE TSUNAMI HAS PASSED.

Fig. 7. Special Weather Statement sent by Eureka National Weather Service (NWS) during the 2011 tsunami.

NATIONAL WEATHER SERVICE EUREKA CA.

AN EARTHQUAKE WITH A PRELIMINARY MAGNITUDE OF 8.9 OCCURRED NEAR THE EAST COAST OF HONSHU, JAPAN AT 11:46 PM PST MAR 10, 2015. IT HAS GENERATED A TSUNAMI. INITIAL WAVES WERE DETECTED AT 08:30 AM PDT MAR 11, 2015. DOCKS HAVE BEEN DESTROYED AT CRESCENT CITY HARBOR. DAMAGING WAVES HAVE BEEN SIGHTED IN HUMBOLDT BAY AND MOVING UP THE MAD RIVER. OTHER WAVES WILL STRIKE OVER MANY HOURS. TSUNAMI WAVES CAN BE DEADLY AND CAUSE INJURY AND WIDESPREAD DAMAGE.

THE TSUNAMI WARNING REMAINS IN EFFECT FOR DEL NORTE, HUMBOLDT, AND MENDOCINO COUNTY COASTAL AREAS. THIS INCLUDES THE TOWNS OF CRESCENT CITY, KLAMATH, EUREKA, ARCATA, TRINIDAD, FORT BRAGG, GUALALA, AND WESTPORT.

IF YOU ARE ON OR NEAR A BEACH, IN A LOW LYING COASTAL AREA, OR NEAR A COASTAL RIVER ANYWHERE IN THE DEL NORTE, HUMBOLDT, AND MENDOCINO COUNTY COASTAL AREAS, YOU WILL BE SAFEST IF YOU IMMEDIATELY GET TO HIGH GROUND OF AT LEAST 50 FEET OR MORE. IF YOU CANNOT REACH HIGH GROUND, EVACUATE TO AN UPPER FLOOR OF A HIGH RISE BUILDING, IF ONE IS AVAILABLE. DO NOT TRAVEL BY WATERCRAFT. TSUNAMI WAVES MAY BE FILLED WITH DEBRIS, WHICH CAN INJURE OR KILL PEOPLE AND WEAKEN OR DESTROY STRUCTURES.

IF YOU SEE THE OCEAN WATER PULL BACK AND EXPOSE THE SEA FLOOR, RUN TO HIGH GROUND AS FAST AS YOU CAN BECAUSE A TSUNAMI WILL STRIKE IN A FEW MOMENTS. IF YOU ARE NOT IN A TSUNAMI IMPACT AREA, STAY AWAY. ONCE YOU ARE IN A SAFE LOCATION, STAY THERE UNTIL ADVISED BY OFFICIALS THAT IT IS SAFE TO LEAVE. KEEP LISTENING TO YOUR LOCAL MEDIA AND EMERGENCY OFFICIALS FOR MORE INFORMATION AND ADDITIONAL UPDATES. IF AVAILABLE, REFER TO TSUNAMI.GOV FOR MORE INFORMATION.

THIS MESSAGE WILL BE UPDATED IN 30 MINUTES OR SOONER.

Fig. 8. Revised tsunami message, based upon findings from the focus groups.

EVACUATE COASTAL AREAS IN MENDOCINO, HUMBOLDT, DEL NORTE COUNTIES.
TSUNAMI WARNING. DESTRUCTIVE WAVES SIGHTED. WARNING EXPIRES 09:00 PM PDT.

Fig. 9. 140-character tsunami message

The findings suggest that the inclusion of more specific data that can be obtained through real-time analysis of secondary scattering phases, such as those illustrated in the ALBACORE array dataset, has the potential to increase message perceptual outcomes among the public in a positive manner. With increased understanding, believing, and personalizing, we expect to see decreased information confirmation activity and a greater likelihood to take protective action. Such results in response to a tsunami message have the potential to save lives under imminent threat conditions.

4. Summary

In this study we used beamforming and back-projection techniques to process the 2011 Tohoku tsunami waveforms recorded by the ALBACORE pressure gauge array off the coast of southern California. We computed the scattering source azimuth of the four coherent tsunami wave arrivals after the first (i.e., direct) arrival with beamforming; we then identified the geographical scatterers that corresponded to these coherent arrivals. The scatters are: (1) southeast Alaska (1–2 hours after the first arrival); and long bathymetry structures near: (2) the northern Hawaiian Island chain (1–2 hours after the first arrival), (3) Papua New Guinea (8–9 hours after the first arrival), and (4) French Polynesia (10–11 hours after the first arrival). Guided by these results, we generated specificity-enhanced message content, assessed by focus groups. The results demonstrate that the inclusion of more specific data that can be obtained

through real-time analysis of secondary scattering phases, such as those illustrated in the ALBACORE array dataset, has the potential to increase message perceptual outcomes among the public in a positive manner. While tsunami impact can be quantified directly by forward simulations without explicitly identifying scatterers, our study outlines a more efficient, simulation-based tsunami early warning approach through ray theory and single-scattering theory (Born approximation). The results shown here pave the way towards this goal.

NWS EUREKA, CA. TSUNAMI WARNING. A MAGNITUDE 8.9 EARTHQUAKE OCCURRED NEAR JAPAN AT 11:46 PM PST MAR 10, 2015. (MESSAGE 1 OF 11)

INITIAL WAVES WERE DETECTED AT 0830 AM PDT MAR 11, 2015. DOCKS HAVE BEEN DESTROYED AT CRESCENT CITY HARBOR. (MESSAGE 2 OF 11)

DAMAGING WAVES HAVE BEEN SIGHTED IN HUMBOLDT BAY AND MOVING UP THE MAD RIVER. OTHER WAVES WILL STRIKE OVER MANY HOURS AND MAY BE DEADLY. (MESSAGE 3 OF 11)

THE TSUNAMI WARNING IS IN EFFECT FOR DEL NORTE, HUMBOLDT & MENDOCINO COUNTY COASTAL AREAS INCLUDING CRESCENT CITY, KLAMATH, EUREKA & ARCATA. (MESSAGE 4 OF 11)

IF YOU ARE ON OR NEAR A BEACH IN A LOW LYING COASTAL OR RIVER TSUNAMI IMPACT AREA, GO NOW TO HIGH GROUND AT LEAST 50 FEET ABOVE SEA LEVEL. (MESSAGE 5 OF 11)

IF YOU ARE IN AN IMPACT AREA AND CANNOT REACH HIGH GROUND, GO TO AN UPPER FLOOR OF A TALL BUILDING. STAY OFF BEACHES. DO NOT USE WATERCRAFT. (MESSAGE 6 OF 11)

TSUNAMI WAVES MAY BE FILLED WITH DEBRIS, WHICH CAN INJURE OR KILL PEOPLE AND WEAKEN OR DESTROY STRUCTURES. (MESSAGE 7 OF 11)

IF YOU SEE THE OCEAN WATER PULL BACK AND EXPOSE THE SEA FLOOR, RUN TO HIGH GROUND AS FAST AS YOU CAN BECAUSE A TSUNAMI IS ABOUT TO STRIKE. (MESSAGE 8 OF 11)

IF YOU ARE NOT IN A TSUNAMI IMPACT AREA, STAY AWAY. ONCE YOU ARE IN A SAFE LOCATION, STAY THERE UNTIL OFFICIALS ADVISE IT IS SAFE TO LEAVE. (MESSAGE 9 OF 11)

LISTEN TO YOUR LOCAL MEDIA AND EMERGENCY OFFICIALS FOR ADDITIONAL TSUNAMI UPDATES. IF AVAILABLE, REFER TO TSUNAMI.GOV FOR MORE INFORMATION. (MESSAGE 10 OF 11)

TSUNAMI WARNING MESSAGES WILL BE UPDATED EVERY 30 MINUTES OR SOONER. (MESSAGE 11 OF 11)

Fig. 10. Sequenced 140-character messages.

5. Acknowledgements

References

[1]   Kohler MD, and Science Team (2010): ALBACORE OBS deployment cruise report. *R/V Melville Cruise MV1010*.

[2]   Kohler MD, and Science Team (2011): ALBACORE OBS recovery cruise report. *R/V New Horizon Cruise NH1111*.

[3]   Cox C, Deaton T, Webb S (1984): A deep-sea differential pressure gauge. *J. Atmos. Oceanic Technol.*, **1**, 246–237.

[4]   González FI, Milburn H, Bernard E, Newman J (1998): Deep-ocean Assessment and Reporting of Tsunamis (DART®): Brief overview and status report. in *Proceedings of the International Workshop on Tsunami Disaster Mitigation, Tokyo, Japan.*

[5]   Meinig C, Stalin S, Nakamura A, Milburn H (2005): Real-time deep-ocean tsunami measuring, monitoring, and reporting system. Tech. Rep., *The NOAA DART II Description and Disclosure*.

[6]   Zhang J, Gerstoft P, Shearer PM (2010): Resolving P-wave travel-time anomalies using seismic array observations of oceanic storms. *Earth and Planetary Science Letters*, **292**, 419–427.

[7]   Meng L, Inbal A, Ampuero J-P (2011): A window into the complexity of the dynamic rupture of the 2011 Mw 9 Tohoku-Oki earthquake. *Geophys. Res. Lett.*, **38,** L00G07, doi:10.1029/2011GL048118.

[8]   Traer J, Gerstoft P, Bromirski PD, Shearer PM (2012): Microseisms and hum from ocean surface gravity waves. *J. Geophys. Res.*, **117**, B11307, doi:10.1029/2012JB009550,

[9]   Heidarzadeh M, Satake K (2014): Possible sources of the tsunami observed in the northwestern Indian Ocean following the 2013 September 24 Mw 7.7 Pakistan inland earthquake. *Geophys. J. Int.*, vol. 199, pp. 752–766.

[10]   Thomson R, Fine I, Rabinovich A, Mihály S, Davis E, Heesemann M, and Krassovski M (2011): Observation of the 2009 Samoa tsunami by the NEPTUNE-Canada cabled observatory: Test data for an operational regional tsunami forecast model. *Geophys. Res. Lett.*, **38** (11).

[11]   Webb SC, Zhang X, and Crawford W (1991): Infragravity waves in the deep ocean. *J. Geophys. Res.*, **96**(C2), 2723-2736.

[12]   Sheehan AF, Gusman AR, Heidarzadeh M, Satake K (2015): Array observations of the 2012 Haida Gwaii tsunami using Cascadia Initiative absolute and differential seafloor pressure gauges. *Seis. Res. Lett.*, **86** (5), 1278–1286.

[13]   Imamura F, Nagai T, Takenaka H, Shuto N (1990): Computer graphics for the study of transoceanic propagation of tsunamis. in *Proceedings of PACON90, Tokyo*, 118–123.

[14]   Nagano O, Imamura F, Shuto N (1991): A numerical model for far-field tsunamis and its application to predict damages done to aquaculture. *Natural Hazards*, **4** (2), 235–255.

[15]   Titov VV, Mofjeld HO, González FI, Newman JC (1999): Offshore forecasting of Alaska-Aleutian Subduction Zone tsunamis in Hawaii. *Tech. Rep., NOAA Technical Memorandum*, ERL **PMEL-114**, 22 pp, PMEL, Seattle, Washington.

[16]   Mofjeld HO, Titov VV, González FI, Newman JC (2001): Tsunami scattering provinces in the Pacific Ocean. *Geophys. Res. Lett.*, **28** (2), 335–338.

[17]   Mofjeld HO, Symons CM, Lonsdale P, González FI, Titov VV (2004): Tsunami scattering and earthquake faults in the deep Pacific Ocean. *Oceanography*, **17** (1), 38–46.

[18]   Borcea L, Papanicolaou G, Tsogka C (2005): Interferometric array imaging in clutter. *Inverse Problems*, **21** (4), 1419–1460.

[19]   Fletcher JB, Spudich P, Baker LM (2006): Rupture propagation of the 2004 Parkfield, California, earthquake from observations at the UPSAR. *Bull. Seis. Soc Am.*, **96** (4B), S129–S142.

[20]   Meng L, Allen RM, Ampuero J-P (2014): Application of seismic array processing to earthquake early warning. *Bull. Seis. Soc Am.*, **104** (5), 2553-2561.

[21]   http://www.geoware-online.com/, commercial software distributor.

[22]   Lin F-C, Kohler MD, Lynett P, Ayca A, Weeraratne D (2015): The March 11, 2011 Tohoku tsunami wavefront mapping across offshore southern California. *J. Geophys. Res.*, **120**, 3350–3362.

[23]   Amante C, Eakins BW (2009): ETOPO1 1 arc-minute global relief model: procedures, data sources and analysis, *NOAA Technical Memorandum NESDIS NGDC-24,* 19 pp.

[24]   Lamb H (1932): *Hydrodynamics*. 6th Edition, Cambridge University Press.

[25]   Mileti DS, Sorensen JH (1990): *Communication of emergency public warnings: A social science perspective and state-of-the-art assessment* (No. ORNL-6609). Oak Ridge National Lab., TN (USA).

[26]   National Research Council (2011): Tsunami warning and preparedness: an assessment of the U.S. tsunami program and the nation's preparedness efforts. National Academies Press. Washington D.C.

[27]   Lindell M K, Prater CS (2010): Tsunami preparedness on the Oregon and Washington coast: Recommendations for research. *Nat. Hazards Rev.,* **11***,* 69-81, doi:10.1061/(ASCE)1527-6988(2010)11:2(69).

[28]   Gregg CE, Ritchie L, Johnston DM, Sorensen J, Vogt-Sorensen B (2014): Recommended revisions to warning product prototypes of the NWS Pacific and West Coast/Alaska Tsunami Warning Centers. NWS Award NA10NWS4670015, ETSU Grant E229101, 30 pp. [Available online at http://nws.weather.gov/nthmp/documents/Warningprototypesreview2014.pdf]